

# Modeling the Galactic CV Distribution for the ChaMPlane Survey

A. B. Rogel

*Physics & Astronomy Department, Bowling Green State University, Bowling Green, OH 43402*

H. N. Cohn, P. M. Lugger

*Astronomy Department, Indiana University, Bloomington, IN 47405*

## ABSTRACT

For purposes of designing targeted cataclysmic variable (CV) detection surveys and interpreting results of other projects with many CV detections such as the ChaMPlane Survey, we have created a model of the CV distribution in the Galaxy. It is modeled as a warped, flared exponential disk with a gaussian vertical distribution. Extinction is based on a detailed Galactic dust and gas model. A luminosity function for CVs is also incorporated, based on a smoothed version of published data. We calculate predicted field detection rates as a function of the limiting magnitude expected for the detecting system (i.e. WIYN/Hydra or NOAO 4m/Mosaic). Monte-Carlo techniques are used to assess statistical fluctuations in these rates. We have created maps of the expected CV distribution for the full non-bulge Galactic plane ( $20^\circ < l < 340^\circ$ ,  $|b| < 15^\circ$ ) for use in both the ChaMPlane Survey and future CV surveys. Assuming a CV distribution with a scale height of 160 pc, the ChaMPlane observational result of 5 CVs in 13 northern fields is best fit by a CV local space density of  $0.9_{-0.5}^{+1.5} \times 10^{-5} \text{pc}^{-3}$ , with the range representing the 95% confidence interval.

*Subject headings:* novae, cataclysmic variables—Galaxy:stellar content—surveys

## 1. Introduction

The ChaMPlane Survey (Grindlay et al. 2005) has as a primary goal the determination of the Galactic cataclysmic variable star (CV) distribution to check if CVs can provide a significant contribution to the diffuse X-ray background of the Galaxy. In the survey design, the local space density of  $10^{-5}$  CVs per cubic parsec (Patterson 1998; Warner 1995) was used

to predict detection rates. Now, with followup WIYN<sup>1</sup>/Hydra spectroscopy acquired for 13 fields, 11 of which are in the second and third Galactic quadrants (Rogel et al. 2006), we may begin to examine the accuracy of the published local CV space density. Also, we seek to make more precise predictions for expected detection rates along various lines of sight by using a more realistic model for the CV distribution within the Galaxy and a detailed model for the gas distribution to compute extinction along the lines of sight.

## 2. The Model

### 2.1. Overview

The basic Monte-Carlo process of determining CV detection rates starts with the creation of a simulated CV population based on adopted models for the Galactic CV radial distribution, vertical distribution, and luminosity function. Input parameters to the model are the local CV density and the CV disk density vertical scale height ( $h_z$ ), with assumed forms for the radial and vertical distributions for the CV population.

The simulated CV population consists of a Galactic position ( $l$ ,  $b$ , and distance) and absolute magnitude for each of  $\sim 2 \times 10^6$  CVs, depending on the input parameters. For each field of interest, the set of CVs that lie in the field is determined. The apparent magnitudes of these CVs are then determined based on both distance and the Galactic extinction derived from the adopted model. A limiting magnitude is applied to obtain a count of detected CVs in each field. We repeat this process 1000 times to assess the statistical fluctuations of the results.

### 2.2. Space distribution

The CV space distribution model is a composite model, with an exponential radial density profile following Binney & Merrifield (1998) Eq. 10.3 (disk only) giving a face-on surface luminosity distribution of  $\Sigma \propto \exp^{-R/R_d}$  with  $R_d = 2.5\text{kpc}$ . The bulge is ignored, as we are primarily looking at fields in the second and third quadrants, so we will never see a significant contribution from bulge CVs. The two first quadrant fields in the Rogel et al. (2006) sample are at galactic longitudes sufficiently far away from the galactic center to avoid

---

<sup>1</sup>The WIYN Observatory is a joint facility of the University of Wisconsin, Indiana University, Yale University, and the National Optical Astronomy Observatories.

the bulge as well. This is *not* the case for the southern hemisphere ChaMPlane spectroscopy done at Magellan and CTIO, as those fields are near the Galactic center and thus likely include bulge CVs (Zhao et al. 2005). The disk model of Robin et al. (2003) was followed to reproduce the warped and flared outer Galactic disk.

To more closely follow the work by Patterson (1984, 1998), which is the source for our preliminary CV detection rates, we use a gaussian density distribution in the  $z$ -direction (Patterson 1984, see §V.c), i.e.  $D \propto \exp^{-[z/h_z]^2}$ . CV scale heights were selected to test the full range of scale heights suggested by Patterson (1984) of 100–250 pc, with an additional test at 300 pc to cover the van Paradijs et al. (1996) suggestion that the scale height is a factor of 2 higher than the 150 pc Patterson (1984) result, which was derived from optically detected CVs. Note that direct comparison of scale heights between Patterson (1984) and van Paradijs et al. (1996) is complicated by the use of a gaussian vertical distribution by Patterson and an exponential vertical distribution by Van Paradijs. Our total test range for the gaussian vertical CV distribution is thus 100-300 pc.

### 2.3. Luminosity distribution

The CV luminosity distribution model is taken from Patterson (1998) Figure 2, with the bright supersoft binaries removed to remove non-accretion powered sources. This leaves only the accretion-powered CV luminosity distribution. A smoothed version of this distribution is used for the model CV population. We adopt a color index of  $V - R = 0.0$  for all CVs. With this assumption, the  $M_V$  given by the luminosity distribution is assumed equal to  $M_R$  used in the apparent magnitude calculation. The true  $V - R$  color of a CV is likely to be redder than this, which would result in an increase in the predicted CV detection rate in the model. As the goal is to make a conservative minimum prediction of CV detections, this choice of CV color is reasonable. As a check of this, all five CV candidates and two previously-known X-ray binaries observed by Rogel et al. (2006) have  $V - R > 0.3$ , with the average  $V - R > 1.0$ .

The magnitudes used by Patterson (1998) to derive the luminosity function are time-averaged values, with the quiescent CV magnitudes being 1-2 magnitudes fainter. Since CVs spend most of the time in the quiescent state, using the time-averaged magnitudes to determine detection will result in an overestimation of CV detections. To eliminate this bias, the luminosity function was dimmed by 1.5 magnitudes to represent a quiescent CV luminosity function. In tests versus a simplistic quiescent/outburst model (90% quiescent, 10% outburst of 3.8 magnitudes brighter, equivalent to a 1.5 magnitude difference between quiescent and time-averaged magnitude), the use of the quiescent luminosity function results

in about a 30% decrease in predicted CV detections. Versus the time-averaged luminosity function, using the quiescent luminosity function results in about a 70% decrease in predicted detections. Clearly, the details of the CV light curve will have a significant impact on detection rates. To investigate this one might draw a random sample of CV luminosities from a known light curve to improve the accuracy of the predicted detections of CVs. However, the differing subtypes of CVs have different outburst behavior and light curve profiles (Warner 1995), necessitating an estimation of the Galactic distribution of each subtype of cataclysmic variable as well as relative numbers of each types. This estimation would add additional uncertainties to the model. Thus, to ensure a conservative minimum prediction for CV detections, the quiescent luminosity function is used in this work.

## 2.4. Extinction Model

The extinction to each simulated CV is determined using the model of Drimmel et al. (2003), due to the full-sky coverage provided by the model. This model uses COBE/DIRBE<sup>2</sup> FIR and NIR data to determine structure and extinction parameters of the Galactic dust distribution. The model calculates  $A_V$  for any location within 15 kpc of the Galactic core. Regions within  $20^\circ$  of the Galactic core are not well modeled. However, this is not an issue in the present work, since all fields are at least  $26^\circ$  in longitude away from the Galactic center. In all cases, the rescaling option included by Drimmel et al. (2003) is used to more closely match the fine structure of the Galactic dust and gas.

Some authors (Arce & Goodman 1999; Cambrésy et al. 2005) have suggested that the Schlegel et al. (1998) data, on which the Drimmel et al. (2003) extinction map is based, may overestimate extinction by a factor of  $\sim 1.3$  for regions where the extinction gradient is low and  $A_V \gtrsim 0.8$ , while possibly underestimating extinction in regions where the extinction gradient is high. We directly examine the case of extinction overestimation below, and see that the resultant change in the overall predicted CV sky density is on the order of 10-20%, which is generally less than other uncertainties in the model. The possibility of extinction underestimation also appears to be limited to relatively small regions of the sky, typically around localized regions of significantly high extinction. However, the localized underestimation seems to be of a similar order to the general overestimation, resulting in similarly modest uncertainties in comparison to others.

---

<sup>2</sup>DIRBE = Diffuse Infrared Background Experiment on NASA Cosmic Background Explorer (COBE).

## 2.5. Other details

Given the high demand for random numbers in the model (5 per CV, several million CVs per model, 1000 model generations), we needed to ensure that our numbers were properly randomized for lists exceeding  $10^{10}$  in length. Therefore, we used the ‘Mersenne Twister’ random number generator MT19937 (Matsumoto & Nishimura 1998)<sup>3</sup>. This generator has a total ‘list length’ of over  $10^{6400}$ , so is easily capable of generating enough random numbers for the model.

## 3. Results

### 3.1. CV Sky-density Maps

The basic model parameters are the scale height of the CV disk, the local CV space density, and the limiting magnitude of detection. For the initial CV sky-density maps, an  $R$ -band limiting magnitude of 22 was selected to correspond to the expected limit for the spectroscopy of the ChaMPlane Survey. A grid was laid down centered on Galactic anticenter with a grid spacing of  $0.6^\circ$  in both  $l$  and  $b$  to correspond to the field of view of the Mosaic imager on the NOAO 4m telescopes used in the ChaMPlane survey. Each simulated CV was then placed (by sky position) into the appropriate field, then checked against the magnitude limit for detection. Averages of CV detections per field were then used to build up the maps.

Figures 1 through 4 are the CV sky-density maps corresponding to four different scale heights spanning the range discussed above. All figures have contours set at unit intervals in predicted CV counts per NOAO 4m Mosaic field. The outermost regions (away from the Galactic plane) all have predicted CV counts of less than one CV per Mosaic field. For clarity, the figures have been stretched by a factor of five in the vertical direction. Note also that these figures, unlike most Galactic-coordinate sky projections, are centered on the Galactic *anticenter*, since the region within  $20^\circ$  of the Galactic center is not modeled. All modeling runs have a local space density set at  $0.6 \times 10^{-5} \text{ pc}^{-3}$ . An important consideration in examining these figures is that the local space density parameter is set at the Galactic plane. This means that an increased scale height (and thus thicker CV disk) requires *more* CVs to populate, thus resulting in generally higher CV numbers, especially away from the Galactic plane. Altering the local space density results in a linear change in the CV sky density, so the maps may be easily scaled to examine other local space densities.

---

<sup>3</sup>[www.math.keio.ac.jp/matsumoto/emt.html](http://www.math.keio.ac.jp/matsumoto/emt.html)

Clearly seen in all maps is the signature of the Galactic warp and the extinction caused by the local Orion Arm at roughly  $l = 80^\circ$  and  $l = 265^\circ$ . Also clear in all cases is the expected general increase in observed CV density as the Galactic longitude of the line of sight approaches the Galactic center. The patchy nature of the maps is due to localized extinction features within the Galactic plane. In all cases, the maximum CV density is located a few degrees (ranging from  $\sim 1.5^\circ$  for  $h_z = 100$  pc to  $\sim 3.5^\circ$  for  $h_z = 300$  pc) below the Galactic plane, due to the gas/dust disk of the Milky Way being substantially thinner than 200 pc, allowing the lines of sight a few degrees off the plane to quickly emerge from the dust disk while still passing through a dense portion of the CV distribution. Only for the thickest ( $h_z = 300$  pc) model does the expected observable CV density become higher than one CV per Mosaic field for Galactic latitudes more than  $\sim 9^\circ$  away from the plane.

### 3.2. ChaMPlane Results

We now apply our model to the northern ChaMPlane fields to test predicted CV detection rates versus the 5 CV detections reported in Rogel et al. (2006). For each ChaMPlane Mosaic field, the model is run to determine a raw number of CVs predicted to be in that field to a specified limiting magnitude. This number must then be reduced to account for survey completeness and known survey selection effects.

#### 3.2.1. ChaMPlane Survey Completeness

Table 1 lists the completion percentage for spectral identification of H $\alpha$ -excess sources in each ChaMPlane field. In summary, we find that spectral identification is about 35% complete to a magnitude of 20.5 for the fields. The completion percentage (columns 5 and 8 of Table 1 is defined to be the fraction of *all* (observed or not) H $\alpha$ -excess sources with spectroscopic identifications. In examining Table 1, it will be noted that the fraction of possible H $\alpha$ -excess targets observed is relatively low in several cases. This is due to the nature of the ChaMPlane Survey, which has as its primary goal the characterization of the X-ray source population in the Galactic plane. H $\alpha$ -excess targets without known X-ray emission were given somewhat reduced priority during spectroscopy. As the Mosaic field of view is  $\sim 4.5$  times larger than the *Chandra* ACIS-I field of view, the X-ray emission status of most H $\alpha$ -excess objects is unknown. However, we find that observed sources have been identified at a success rate of 87% to a limiting magnitude of 20.5, indicating both a high success rate at identifying sources and a significant need for further data. For a limiting magnitude of 22.0, the total identification success rate falls to 75%, with identification success

of 55% for objects within the magnitude range 20.5-22. This is attributed mainly to G-type stars which have few prominent spectral features (the Na D line is heavily contaminated by skylight, and thus is not used in our spectral identification). We would expect to still be able to spectroscopically identify CVs in this dimmer magnitude range due to typically broad, strong  $H\alpha$  emission features. The five CV candidates identified by Rogel et al. (2006) have magnitudes in the range 19.3 to 21.6, which supports this expectation. The dimmest objects identified for each field have magnitudes ranging from 21-23. We therefore look at two limiting magnitude cases: one at 20.5 for near-certain spectral identification (which would guarantee CV identification), and another at 22.0 for possible CV identification.

### 3.2.2. Selection Effects

The main selection effect in the ChaMPlane Survey to consider is the use of a color selection threshold of  $H\alpha - R < -0.3$  for potential  $H\alpha$ -excess emission objects, which corresponds to an  $H\alpha$  emission line equivalent width of  $28\text{\AA}$ . As CVs are generally accretion-powered sources, they typically have  $H\alpha$  emission. To date, there is no comprehensive catalog of emission-line equivalent widths for CVs, and even finding published values for  $H\alpha$  proved challenging ( $H\beta$  is more commonly cited). However, Liu et al. (1999), Williams (1983), and Zwitter & Munari (1994) each report  $H\alpha$  equivalent widths for a selection of CVs, obtained in studies to spectroscopically confirm the identity of candidate CVs. Combining data from these three spectral surveys allows for an estimation of the fraction of CVs with  $H\alpha$  emission line strengths below the ChaMPlane threshold value. In total,  $\sim 42\%$  of the CVs in the three surveys had equivalent widths greater than  $28\text{\AA}$ ,  $\sim 7\%$  had multiple equivalent widths reported with values on both sides of the cutoff, and  $\sim 50\%$  had no equivalent width reported above the cutoff. Thus, allowing for some variability as seen in multi-epoch data in the surveys, it seems reasonable to conclude that about half of available CVs in ChaMPlane fields would have sufficiently strong  $H\alpha$  emission to be included as targets for spectroscopic identification under ChaMPlane protocols. An equivalent width of  $28\text{\AA}$  should produce a readily-visible feature even at faint magnitudes as discussed above. An additional small fraction of CVs would be selected as targets based on X-ray emission, but as the *Chandra* ACIS-I field of view is  $\sim 20\%$  the size of the Mosaic field, this will add back only a few percent of CVs lost due to low  $H\alpha$  emission, leaving the 50% estimate of available CVs actually being targeted by ChaMPlane spectroscopy essentially unchanged.

### 3.2.3. Results

Table 2 gives the total model predictions (after taking into account field completeness and the  $H\alpha$  line strength selection effect) for the 13 ChaMPlane fields with WIYN spectroscopy reported in Rogel et al. (2006). Four scale heights were examined in the model, along with two limiting magnitudes. The model was run a total of 1000 times for each field to generate the statistics. The standard deviations quoted are computed directly from the Monte-Carlo results of the model for each field, then combined in quadrature to get a net uncertainty. Two fields, MWC297 and SGR1900, are of concern in this work; SGR1900 due to short exposure times during photometry and MWC297 due to the presence of the Herbig-Haro Be star MWC297 and associated local gas and dust in the field, which is likely to produce anomalous extinction results as discussed by Drimmel et al. (2003). An examination of the  $R$ -band image for MWC297 clearly shows significant ( $> 5$  magnitude) extinction across more than half the image. Included in table 2 are results based on both all 13 ChaMPlane fields and for all fields but these two. Based on these results, and assuming a CV distribution with a scale height of 160 pc, the ChaMPlane observational result of 5 CVs in 13 northern fields is best fit by a CV local space density of  $0.9_{-0.5}^{+1.5} \times 10^{-5} \text{pc}^{-3}$ , with the range representing the 95% confidence interval. Figure 5 plots local space density versus scale height and shows the range of possible values consistent with the ChaMPlane results to one standard deviation (shaded regions) and two standard deviations (lines), indicating the need for a higher local space density as the scale height decreases. The Patterson (1984) local CV space density is consistent within two standard deviations of the ChaMPlane results for all scale heights. At the low end of the scale height range, the prediction is just less than  $2\sigma$  above the Patterson (1984) value. This is also in agreement with the suggestion of Grindlay et al. (2005) that the CV local space density derived from the *ROSAT* Bright Star Survey (Schwope et al. 2002) and the earlier *Einstein* Galactic Plane Survey (Hertz et al. 1990) of  $3 \times 10^{-5} \text{pc}^{-3}$  is too high by a factor of  $\sim 3$ . A recent study of results from the *ROSAT* North Ecliptic Pole survey (Pretorius et al. 2007) is also in agreement with our predictions.

### 3.3. Modifications to Extinction

As noted previously, the Drimmel et al. (2003) model may overestimate extinction in areas where  $A_V$  is high. To check the effect of this, the model was adjusted to use the Cambr esy et al. (2005) extinction modification of

$$A_{V(\text{Cambr esy})} = \frac{A_{V(\text{Drimmel})} + 0.24}{1.31}$$

if  $A_V(\text{Drimmel}) > 0.774$ , which is the extinction for which the Cambr sy et al. (2005) and Drimmel et al. (2003)  $A_V$  values are equal. For comparison, the model was run for ChaMPlane fields with scale height of 160 pc. For the 11 true anticenter fields, the average increase in predicted CVs was 8%. This is a negligible increase, considering the uncertainty in the best-fit CV local space density cited above. The two quadrant 1 fields, MWC297 and SGR1900, had higher changes, with SGR1900 predicted CVs up by 45% and MWC297 predicted CVs up by 73%. However, the MWC297 field has a visible strong extinction gradient as noted above, which could lead to the Drimmel et al. (2003) extinction being an underestimate rather than an overestimate. The location of the SGR1900 field at ( $l = 43^\circ, b = +0.8^\circ$ ), very close to the galactic plane, may also experience a high extinction gradient, so CV predictions there are possibly inflated as well. Including these fields in the comparison results in a 18% increase in predicted CVs, still a small contribution to the total [model uncertainty] [change when compared to the CV local space density uncertainty.] Other ChaMPlane fields are not expected to be at locations with high extinction gradients, because the regions of high extinction gradient noted in Arce & Goodman (1999), where the Drimmel et al. (2003) model is shown to underestimate  $A_V$ , are all in regions of high  $A_V$ . ChaMPlane fields were specifically selected to have low  $A_V$ , so problematic locations have generally been avoided in the ChaMPlane Survey. A more recent extinction model, taking into account the concerns of Cambr sy et al. (2005) and Arce & Goodman (1999), would be beneficial for this work, in particular for the all-sky maps. The model of Marshall et al. (2006) appears to avoid the potential shortcomings of the Drimmel et al. (2003) model, but as it only covers  $|l| < 100^\circ$ , much of the current model’s sky coverage is not included, including 11 of 13 ChaMPlane fields. Thus, for the present application of the model to ChaMPlane results, the Marshall et al. (2006) model is insufficient. However, as the CV density is clearly highest in quadrants 1 and 4, we plan to compare predictions of the model based on the Drimmel et al. (2003) extinction and a limited sky coverage version of the model using the Marshall et al. (2006) extinction model to examine the potential effects of this extinction underestimation on predictions made for future targeted CV surveys.

#### 4. Conclusion

Based on the model of the disk CV distribution presented here, it appears that the ChaMPlane Survey CV detections reported in Rogel et al. (2006) for 13 northern WIYN-surveyed fields are consistent with a CV density of  $0.6 \times 10^{-5} \text{pc}^{-3}$  and the range of scale heights proposed by Patterson (1984). This also supports the suggestion of Grindlay et al. (2005) that earlier *ROSAT* and *Einstein* derived CV space densities of  $3 \times 10^{-5} \text{pc}^{-3}$  are too high by a factor of  $\sim 3$ . Completion of spectroscopic identification of potential targets in the

ChaMPlane fields will result in much smaller viable ranges for the local space density and scale heights of CVs, narrowing the allowable parameter space. The model will also allow future survey projects to selectively target potentially high-output fields to significantly boost the number of new CV detections, thus allowing for further investigations of both the spatial distribution of CVs and also the CV luminosity function.

This research was supported in part by NSF grant AST-0098683 and NASA/Chandra grants AR2-3002B, AR3-4002B, and AR4-5003B to Indiana University. Additional support was provided by NASA through the American Astronomical Society’s Small Research Grant Program. Finally, ABR gratefully acknowledges a Fellowship from the Indiana Space Grant consortium.

## REFERENCES

- Arce, H. G., & Goodman, A. A. 1999, *ApJ*, 512, 135
- Binney, J., & Merrifield, M. 1998, *Galactic Astronomy* (Princeton: Princeton University Press)
- Cambrésy, L., Jarrett, T. H., & Beichman, C. A. 2005, *A&A*, 435, 131
- Drimmel, R., Cabrera-Lavers, A., Lopez-Corredoira, M. 2003, *A&A*, 409, 205
- Grindlay, J., et al., 2005, *ApJ*, 635, 920
- Hertz, P., Bailyn, C. D., Grindlay, J. E., Garcia, M. R., Cohn, H., & Lugger, P. M. 1990, *ApJ*, 364, 251
- Liu, W., Hu, J. Y., Zhu, X. H., & Li, Z. Y., 1999, *ApJS*, 122, 243
- Marshall, D. J., Robin, A. D., Reylé, C., Schultheis, M., & Picaud, S. 2006, *A&A*, 453, 635
- Matsumoto, M., & Nishimura, T. 1998, *ACM Trans. on Modeling and Computer Simulation* Vol. 8, No. 1, 3
- Patterson, J. 1984, *ApJS*, 54, 443
- Patterson, J. 1998, *PASP*, 110, 1132
- Pretorius, M. L., Knigge, D., O’Donoghue, D., Henry, J. P., Gioia, I. M., & Mullis, C. R., *MNRAS*, in press, (astro-ph/arXiv:0709.1887v1)

- Robin, A. C., Reyle, C., Derriere, S., & Picaud, S. 2003, *A&A*, 409, 523
- Rogel, A. B., Cohn, H. N., Lugger, P. M., Slavin, S. D., Grindlay, J. E., Zhao, P., & Hong, J. 2006, *ApJS*, 163, 160
- Schlegel, D. J., Finkbeiner, D. P., & Davis, M. 1998, *ApJ*, 599, 525
- Schwope, A. D., Brunner, H., Buckley, D., Greiner, J., Heyden, K. v. d., Neizvestny, S., Potter, S., & Schwarz, R. 2002, *A&A*, 396, 895
- van Paradijs, J., Augusteijn, T., & Stehle, R. 1996, *A&A*, 312, 93
- Warner, B. 1995, *Cataclysmic Variable Stars* (Cambridge: Cambridge Univ. Press)
- Williams, G. 1983, *ApJS*, 53, 523
- Zwitter, T. & Munari, U., 1994, *A&A*, 107, 503
- Zhao, P., Grindlay, J. E., Hong, J., Laycock, S., Koenig, X. P., Schlegel, & van den Berg, M. 2005, *ApJS*, 161, 429

Table 1. ChaMPlane Field Completion Rate

Field	CV <sup>a</sup>	16.0 to 20.5 mag. <sup>b</sup>			16.0 to 22.0 mag. <sup>b</sup>		
		Targ. <sup>c</sup>	Obs. <sup>d</sup>	ID'd <sup>e</sup>	Targ. <sup>c</sup>	Obs. <sup>d</sup>	ID'd <sup>e</sup>
3C 123	1	0	0	...	4	3	50.0%
3C 129	0	3	1	33.3%	10	6	40.0%
GK Persei <sup>f</sup>	0	6 <sup>f</sup>	0	0.0%	78 <sup>f</sup>	2	2.6%
NGC 1569	0	9	2	0.0%	35	3	2.9%
without core <sup>g</sup>	0	3	2	0.0%	4	2	0.0%
J2227+6122	0	11	10	54.5%	14	12	50.0%
SGR1900+14	0	109	31	28.4%	163	38	22.1%
B2224+65	0	5	5	100.0%	11	7	54.5%
J0422+32	1 <sup>h</sup>	2	2	50.0%	8	8	50.0%
A0620-00	0	2	2	100.0%	21	12	47.6%
MWC297	1 <sup>h</sup>	57	19	33.3%	67	21	28.4%
G116.9+0.2 <sup>i</sup>	1 <sup>h</sup>	11 <sup>i</sup>	4	27.3%	120 <sup>i</sup>	10	4.2%
PSRJ0538+2817	0	4	4	50.0%	19	9	15.8%
M1-16	1	0	0	...	83	4	2.4%

<sup>a</sup>Number of new CV candidates in field.

<sup>b</sup>R-band magnitude range of target list.

<sup>c</sup>Total number of H $\alpha$ -excess objects in field.

<sup>d</sup>Number of observed H $\alpha$ -excess objects in field.

<sup>e</sup>Percentage of all targets (observed or not) with spectral identifications.

<sup>f</sup>Many ‘sources’ are due to the GK Persei nova shell.

<sup>g</sup>Statistics without sources located in the core of NGC 1569

<sup>h</sup>CV candidates with magnitudes less than 20.5.

<sup>i</sup>Many ‘sources’ are due to H $\alpha$  filaments of a supernova remnant.

Table 2. ChaMPlane Field Predicted CV Detection Rates

Scale height	Fields	Lim. Mag	Predicted Detections <sup>a</sup>	Standard Deviation	Actual Detections
100 pc	13 <sup>b</sup>	20.5	1.2	1.1	3
...	...	22.0	2.3	1.5	5
...	11 <sup>c</sup>	20.5	1.0	1.0	2
...	...	22.0	1.7	1.3	4
160 pc	13 <sup>b</sup>	20.5	1.8	1.3	3
...	...	22.0	3.3	1.8	5
...	11 <sup>c</sup>	20.5	1.5	1.2	2
...	...	22.0	2.6	1.6	4
230 pc	13 <sup>b</sup>	20.5	2.4	1.6	3
...	...	22.0	4.1	2.0	5
...	11 <sup>c</sup>	20.5	2.1	1.5	2
...	...	22.0	3.4	1.9	4
300 pc	13 <sup>b</sup>	20.5	2.9	1.7	3
...	...	22.0	5.0	2.2	5
...	11 <sup>c</sup>	20.5	2.6	1.6	2
...	...	22.0	4.1	2.0	4

For a local space density of  $0.6 \times 10^{-5} \text{pc}^{-3}$

<sup>a</sup>Factoring in completeness fraction of observations and EW(H $\alpha$ ) selection effect.

<sup>b</sup>All 13 ChaMPlane fields.

<sup>c</sup>SGR1900 field removed due to short exposures for photometry and resulting uncertainties, MWC297 field removed due to model extinction concerns due to Herbig-Haro Be star MWC297.

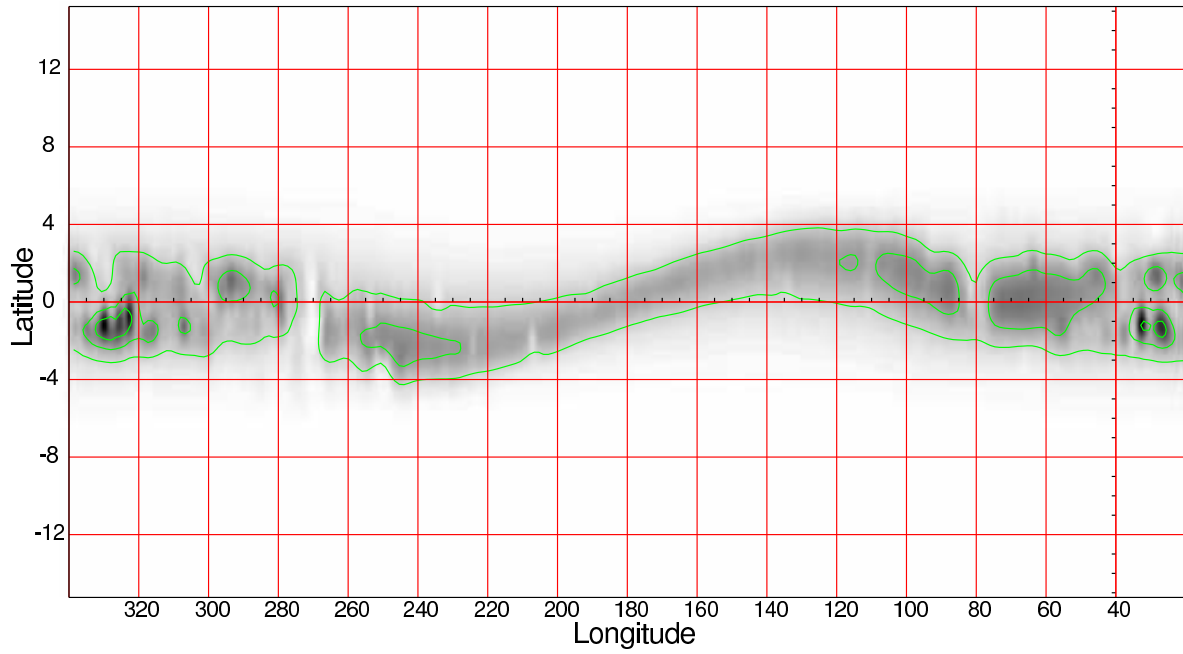


Fig. 1.— Predicted CV detection rate vs. Galactic coordinates.  $R < 22.0$ , scale height  $h = 100$  pc. The detection rate is in units of CV per  $0.36^\circ$  square degree field. Contour levels start from one CV per field and are at unit intervals. *See the electronic edition of the Journal for a color version of this figure.*

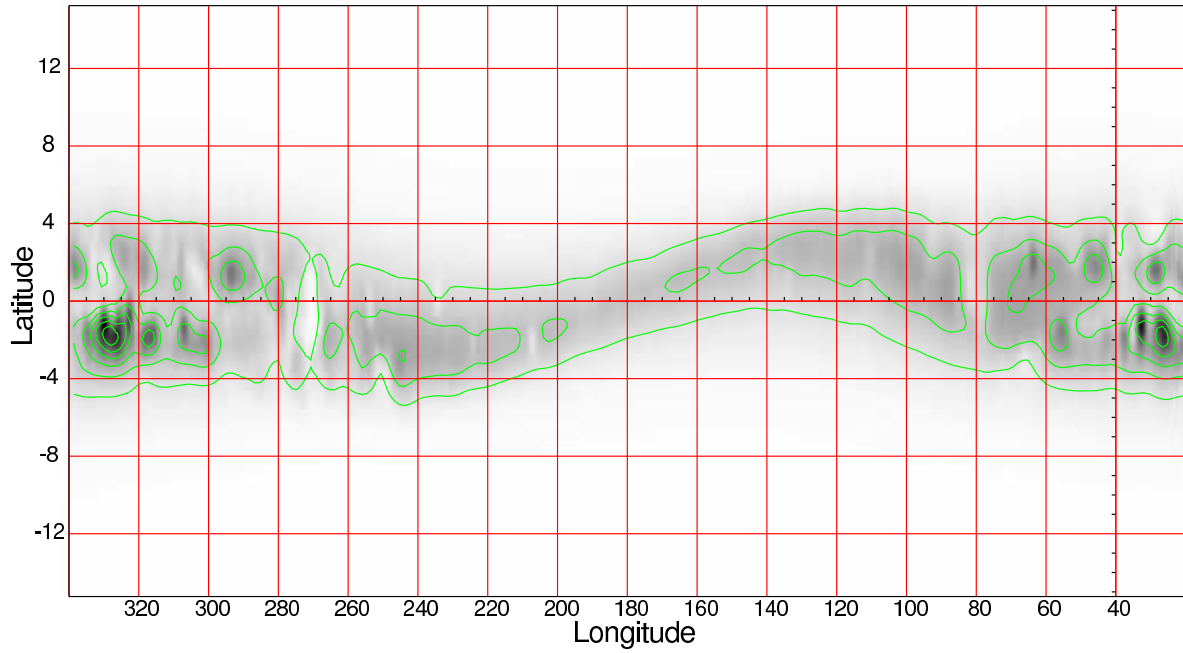


Fig. 2.— Predicted CV detection rate vs. Galactic coordinates, as for Figure 1.  $R < 22.0$ , scale height  $h = 160$  pc. See the electronic edition of the *Journal* for a color version of this figure.

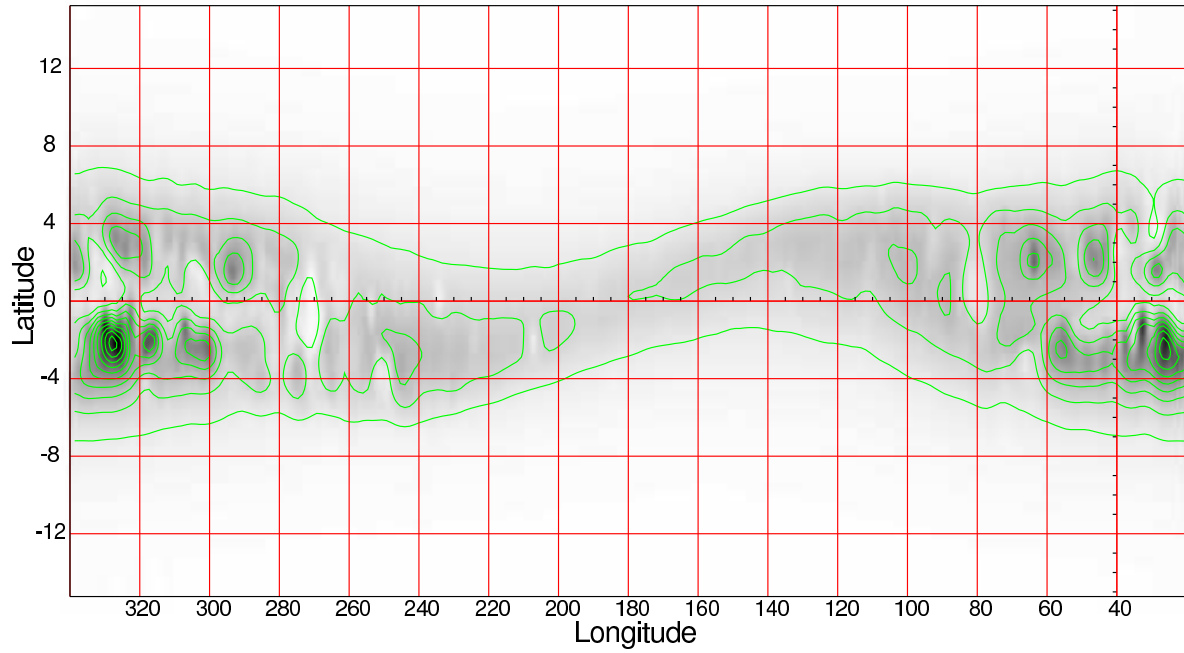


Fig. 3.— Predicted CV detection rate vs. Galactic coordinates, as for Figure 1.  $R < 22.0$ , scale height  $h = 230$  pc. See the electronic edition of the *Journal* for a color version of this figure.

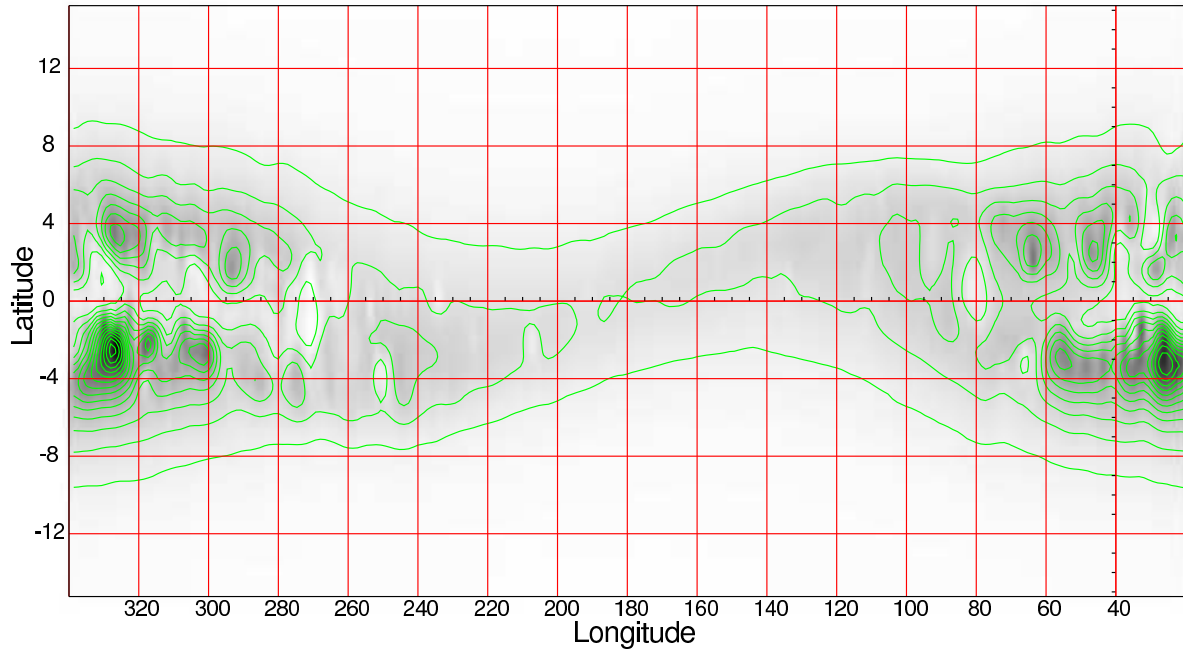


Fig. 4.— Predicted CV detection rate vs. Galactic coordinates, as for Figure 1.  $R < 22.0$ , scale height  $h = 300$  pc. See the electronic edition of the *Journal* for a color version of this figure.

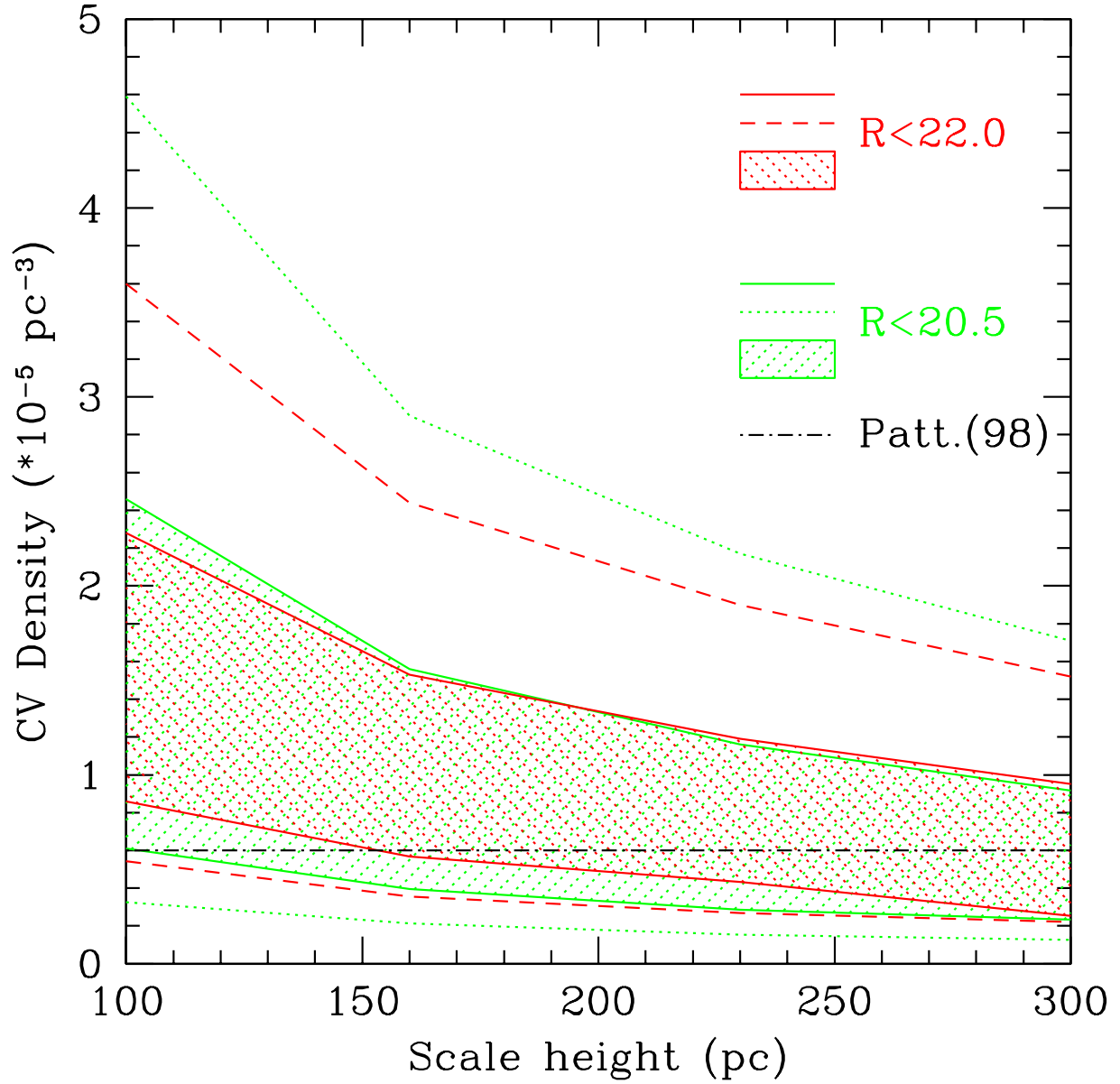


Fig. 5.— Scale height vs. CV space density. The shaded regions represent the  $1\sigma$  error limit for the two different limiting magnitudes, while the dashed/dotted lines show the  $2\sigma$  error limits. The horizontal dot-dash line is the Patterson (1984) CV space density. *See the electronic edition of the Journal for a color version of this figure.*